



Visualization of Rostral Migratory Stream in the Developing Rat Brain by In Vivo Electroporation

Yi-wei Xie¹ · Zhao-yun Li⁴ · Jing Du¹ · Yu Chen¹ · Bing-yu Chen¹ · Tong-tong Wang¹ · Zhihui Huang² · Shuangxing Hou³ · Ying Wang¹

Received: 16 September 2017 / Accepted: 6 February 2018 / Published online: 13 February 2018
© Springer Science+Business Media, LLC, part of Springer Nature 2018

Abstract

Interneurons in the olfactory bulb (OB) are generated from neuronal precursor cells migrating from anterior subventricular zone (SVZa) not only in the developing embryo but also throughout the postnatal life of mammals. In the present study, we established an in vivo electroporation assay to label SVZa cells of rat both at embryonic and postnatal ages, and traced SVZa progenitors and followed their migration pathway and differentiation. We found that labeled cells displayed high motility. Interestingly, the postnatal cells migrated faster than the embryonic cells after applying this assay at different ages of brain development. Furthermore, based on brain slice culture and time-lapse imaging, we analyzed the detail migratory properties of these labeled precursor neurons. Finally, tissue transplantation experiments revealed that cells already migrated in subependymal zone of OB were transplanted back into rostral migratory stream (RMS), and these cells could still migrate out tangentially along RMS to OB. Taken together, these findings provide an in vivo labeling assay to follow and trace migrating cells in the RMS, their maturation and integration into OB neuron network, and unrecognized phenomena that postnatal SVZa progenitor cells with higher motility than embryonic cells, and their migration was affected by extrinsic environments.

Keywords Olfactory bulb · Rostral migratory stream · Interneurons · Migration · In vivo electroporation

Yi-wei Xie, Zhao-yun Li, and Jing Du have contributed equally to this work.

Electronic supplementary material The online version of this article (<https://doi.org/10.1007/s10571-018-0577-6>) contains supplementary material, which is available to authorized users.

- ✉ Zhihui Huang
hzhzju021@163.com
- ✉ Shuangxing Hou
housx021@163.com
- ✉ Ying Wang
nancywangying@163.com

- ¹ Department of Transfusion, Zhejiang Provincial People's Hospital, People's Hospital of Hangzhou Medical College, Hangzhou 310014, China
- ² Wenzhou Medical University, Institute of Neuroscience, Wenzhou 325035, Zhejiang, China
- ³ Department of Neurology, Shanghai Pudong Hospital, Fudan University Pudong Medical Center, 2800 Gongwei Road, Pudong 201399, Shanghai, China
- ⁴ Department of Clinical Laboratory, Taizhou Central Hospital (Taizhou University Hospital), Taizhou 318000, Zhejiang, China

Introduction

Neuronal migration is crucial for brain development, and its migratory defects are leading to neurological disease such as epilepsy and mental retardation (Ayala et al. 2007). Neuroblast migration from anterior sub-ventricular zone (SVZa) to olfactory bulb (OB) through rostral migratory stream (RMS) has been defined as tangential “chain migration” similar to chain migration of neural crest cells during development (Kulesa and Fraser 2000). In human infancy, neuroblast migration along RMS is prominent, and is believed to play an important role in this crucial stage of brain development (Sanai et al. 2011). In adulthood, human SVZ-derived neuroblasts migrate towards striatum, and this process is impaired in some human diseases such as Huntington's disease patients (Ernst et al. 2014). This continuous supply of new neurons in the OB is implicated in plasticity and memory regulation (Sakamoto et al. 2014).

In mammals, interneuron production in the olfactory bulb (OB) begins as early as embryonic day E14 in mice (Wichterle et al. 2001) and is persistently generated throughout the life (Lledo et al. 2008). New OB interneurons

originate from SVZa, a restricted germinal region of SVZ surrounding the anterior part of lateral ventricles (Alvarez-Buylla and Lim 2004; Luskin 1993). The unique neural progenitor cells there, referred to as SVZa cells, or type A cells, form chains ensheathed by astrocytes and migrate tangentially to form the RMS leading into middle of OB. After migration tangentially through RMS, neuroblast cells migrate radially into granule and periglomerular layers of OB, in which they differentiate and mature into various subtypes of local inhibitory interneurons that integrate into the existing circuitry (Pencea et al. 2001; Fasolo et al. 2002; Coskun and Luskin 2002). The long-standing observation showed that the chain orientation was stable and deterministic (Luskin 1993; Luskin et al. 1997), but the brain slices observation of EGFP⁺ mice showed that the migrating cells displayed complex local motility (Martinez-Molina et al. 2011). Although several methods such as dye or BrdU injection or in vivo electroporation (Boutin et al. 2008; Dixon et al. 2017; Sonogo et al. 2015; Bakhshetyan and Saghatel'yan 2015) have been developed to label these neuroblasts and some molecules have been identified to regulate migration of neuroblasts (Kaneko et al. 2017; Sonogo et al. 2015; Omori et al. 2015; Lalli 2014; Persson et al. 2013; Lindberg et al. 2012), it remains unclear that the difference of migratory properties of neuroblasts generated at between embryonic and postnatal ages and how intrinsic or extrinsic factors regulate neuroblast migration in OB.

In present study, we established an in vivo electroporation assay to label RMS of rat both at embryonic and postnatal ages. Based on this assay and time-lapse imaging assay, we could label and identify the migratory behavior of a population of SVZa progenitors to follow their migration pathway and later differentiation in the OB. We found the labeled cells displayed high motility and postnatal generated cells migrate faster than the embryonic generated ones. Our studies will provide a powerful tool and some insights to understand the migratory properties and molecular mechanisms of neuroblasts in RMS at embryonic and postnatal ages.

Materials and Methods

Animals

Sprague–Dawley (SD) rats were provided by Wenzhou Medical University Animal Core Facility. The authors stated that all experimental methods involving rats were carried out in accordance with relevant guidelines and regulations of the Animal Bioethics Committee of Wenzhou Medical University, and all experimental protocols involving rats were approved by Animal Bioethics Committee of Wenzhou Medical University.

In Vivo Electroporation

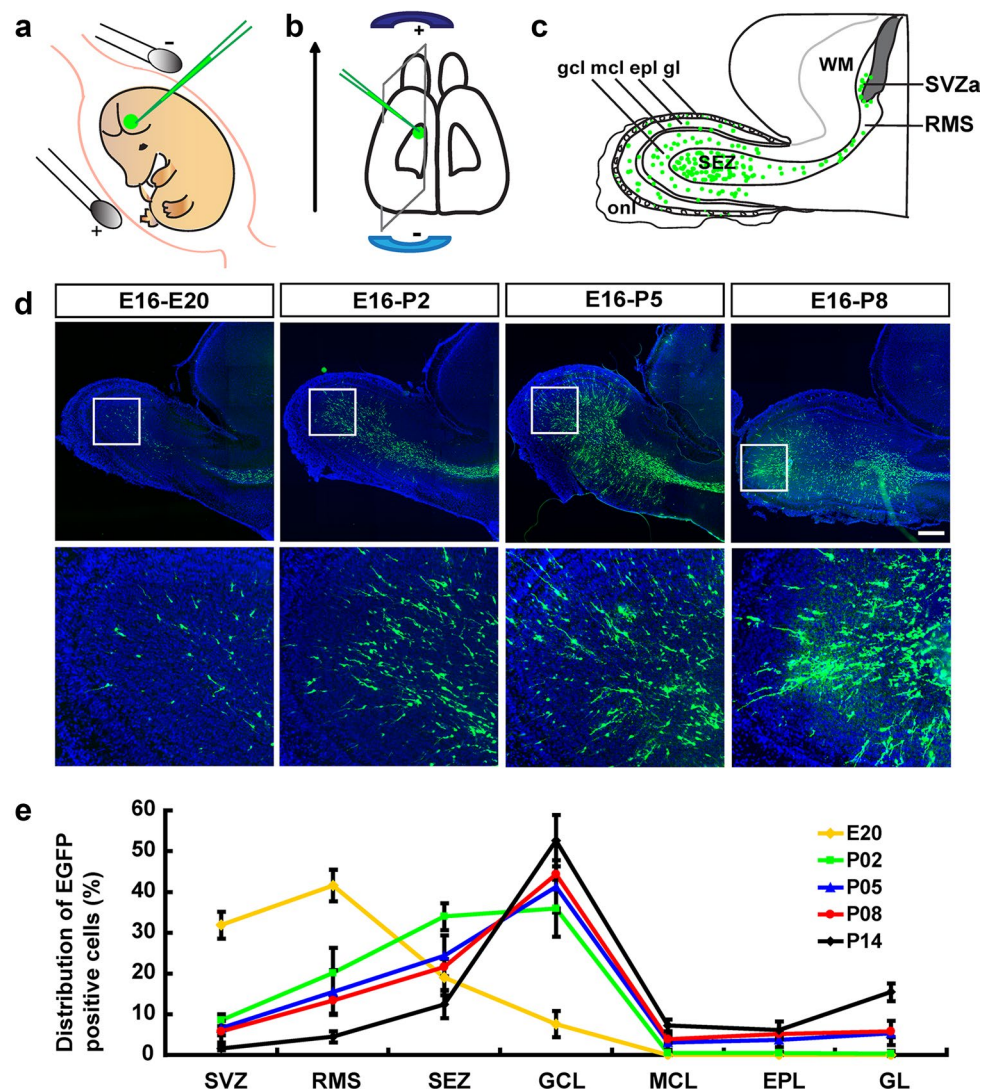
For embryonic manipulation, in utero electroporation was used to introduce EGFP (with CAG promoter) plasmid into SVZ as described previously (Chen et al. 2008). Briefly, SD rats at 16 d of gestation (E16) were deeply anesthetized with 10% chloral hydrate (3.5 ml/kg of body weight) intraperitoneally. After uterus were exposed, 1 μ l of EGFP plasmid (3 μ g/ μ l) mixed with 1 μ l Fast Green (1 μ g/ μ l; Sigma) was injected by trans-uterus pressure microinjection into the anterior part of lateral ventricle of embryos. Fast Green dyes diffused in the ventricle and labeled ventricle, and formed “half-moon”-like structure in the brain surface. Next, the embryos were placed between tweezer-type electrodes anterior-posteriorly, which has disk electrodes of 5 mm in diameter at the tip. The electric pulses were generated by an Electro Squire Porator T830 (BTX) and applied to anterior part of brain at five repeats of 60 V for 50 ms, with an interval of 100 ms (as shown in Fig. 1). Then the uterine horns were placed back into the abdominal cavity to allow embryos to continue normal development. The survival percentage of mother rats was about 93%.

For postnatal manipulation, SD rats at postnatal 1 d were anesthetized on ice, and EGFP plasmid with Fast Green was injected by *trans*-uterus pressure microinjection into the anterior part of lateral ventricle. The head of postnatal rat was placed between tweezer-type electrodes anterior-posteriorly. The electric pulses were generated at five repeats of 60 V for 50 ms, with an interval of 100 ms. Skin was suture-closed. Pups (more than 93%) were then reanimated and returned to their mother to continue normal development.

Immunostaining

After transcardial perfusion at appropriate ages, rat brains were collected and fixed in 4% paraformaldehyde (PFA). After washing in PBS for 1 h, the samples were equilibrated in 30% sucrose (Sigma) in PBS. For fluorescence immunostaining, fixed brains were cryopreserved in OCT compound (Sakura) and frozen in liquid carbon dioxide. Sagittal or coronal cryostat sections of 20–30 μ m were cut on a freezing microtome (Leica) and immediately processed for immunostaining by a three-step free-floating protocol (at 4 °C). In brief, after washing with PBS, sagittal or coronal cryostat sections were permeabilized with 0.3% Triton X-100 in 0.1 M PBS for 30 min, followed by incubation in blocking buffer (5% normal goat serum in PBS, pH 7.4) for 1 h, and incubated overnight at 4 °C with

Fig. 1 Migration pattern of SVZa progenitor cells to the OB. **a–c** Illustration of in utero electroporation strategy to study RMS. Big green dots **a–b** indicated the injected EGFP plasmids. Blue shapes **b** indicated electrode position. Small green dots **c** indicated progenitor cells transfected with GFP migrated from SVZa to OB. **d** Sagittal rat forebrain slice immunostained for GFP at different stages after electroporation of a GFP-expressing plasmid in E16 SVZa cells. SVZ-derived migrating neuroblasts were visible along the RMS and some of them reached the OB. Selected regions were shown at higher magnification. **e** Quantification of GFP-positive cells distribution in RMS pathways at different developmental stages ($n = 10$). SVZ: subventricular zone; RMS: rostral migratory stream; SEZ: subependymal zone; GCL: granule cell layer; EPL: external plexiform layer; GL: glomerular layer; OB: olfactory bulb; ONL: olfactory nerve layer; WM: white matter; MCL: mitral cell layer. Scale bars, 200 μm . Data were mean \pm sem



primary antibodies diluted in the blocking buffer. Sections were washed three times with PBS and incubated for 1 h at room temperature with an appropriate fluorescence-conjugated secondary antibody (1:1000, Molecular probe, Eugene, OR), and incubated with 4', 6'-diamidino-2-phenylindole (DAPI, Sigma, 1:5000) for 45 min, and then visualized by Neurolucida (Microbright field) or confocal microscope (FV1000, Olympus). The primary antibodies and their appropriate concentration used in this experiment were as follows: anti-GFP (1:1000, polyclonal, Molecular probe); anti-Tuj1 (1:2000, polyclonal, Sigma); anti-GFAP (1:500, polyclonal, DAKO); anti-GAD65/67 (1:500, polyclonal, Sigma); anti-MAP2 (1:1000, polyclonal, Millipore); anti-NG2 (1:500, polyclonal, Millipore); anti-NeuN (1:500, monoclonal, Millipore); anti-PSA-NCAM (1:200, monoclonal, Millipore); anti-nestin (1:500, monoclonal, Millipore).

Slice Culture

Slice culture was prepared from P3 to P7 rats and maintained in culture as described previously (Chen et al. 2008). Briefly, brains were dissected out in ice-cold Hanks' balanced salt solution (HBSS), embedded in 4% low-melting point agarose in HBSS, and sectioned (sagittal) on a vibratome at 300 μm thickness. Slices were cultured on a transparent porous membrane (0.4 μm pore size; Millipore) in a six-well culture plate containing 1 ml medium (DMEM plus 10% horse serum; Gibco), and were cultured in a 37 $^{\circ}\text{C}$, 5% CO_2 incubator.

Time-Lapse Imaging

Brains were transfected with EGFP at P0–P1 and sectioned (sagittal) on a vibratome at 300 μm thickness at P3 in ice-cold HBSS as described above. Slices were transferred to

the surface of a transparent porous membrane (0.4 μm pore size; Millipore) in a 35-mm culture dish containing 1 ml of medium (DMEM plus 10% horse serum; Gibco). The culture dish was then sealed with parafilm and transferred to a heat stage (37 °C) on the confocal microscope (FV1000, Olympus). Frames were obtained every 5 min, during 3–4 h without interruption.

Cell Measurements and Quantification

The numbers of transfected cells in the slices were measured from all sections containing EGFP-labeled cells using NeuroLucida (Microbright field). EGFP-labeled cells on brain sections were counted across different zones at different developmental stages, and distribution of transfected cells was analyzed using the software image-Pro plus 5.1. At least 10 Sects. (1 section per rat) were counted for each experiment.

Statistical Analysis

Data were analyzed with SPSS software 17.0 and Excel software (2016). Statistical analysis was performed using Student's *t* test. Statistical significance was defined as $p < 0.05$.

Results

Migration Pattern of SVZa Progenitor Cells to the OB

To study the migration pattern of SVZa cells, progenitor cells at the anterior wall of SVZ enveloping lateral ventricles of rat brain at embryonic day 16 (E16) were transfected with a plasmid encoding enhanced green fluorescent protein (EGFP) by in utero electroporation (Fig. 1a, b). The locations of EGFP-marked cells were examined after transfection. We found these transfected cells (EGFP positive) began to migrate and form a restricted stream of cells extending from SVZa to OB, as shown in Fig. 1c, d. The route of these EGFP-marked cells coincides with the path which is darkly staining region by DAPI, which suggest RMS with highly dense cells (Fig. 1d).

At E20, most EGFP-positive cells stayed at the SVZa, maybe undergoing further division. However, as early as at P2, 40% EGFP-positive cells began to migrate out of SVZa and formed the original RMS pathway. Some cells with high motility even reached the middle of OB (Fig. 1d, e). At P2, almost 90% of transfected cells were restricted in the RMS pathway. Almost 70% cells entered subependymal zone (SEZ) to begin to migrate perpendicularly (Fig. 1d, e).

At P5, even more EGFP⁺ cells had migrated into OB, and 40% cells migrated into granule cell layer (GCL), and some cells even reached the mitral cell layer (MCL), the

external plexiform layer (EPL), and the glomerular layer (GL). Some cells arrived at the border of SEZ, attended a longer leading process, and formed a right angle turn out of SEZ, perpendicularly to the margin of OB, exhibiting a radial pattern (Fig. 1d, e). These suggest that the cells began to change their migration pattern from tangential to radial once they arrived at SEZ of OB, by changing the direction of leading process.

At P8, RMS route from SVZa to SEZ started to become smaller, and almost 90% EGFP⁺ cells detached from the chain and began their radial migration in the OB, and more cells entered GCL, MCL, EPL, and GL. At P14, EGFP⁺ cells were widely dispersed in the OB, toward radially into superficial layer of OB. More EGFP⁺ cells migrated into more superficial layers, and mainly concentrated at the GCL and GL, where the two major classes of OB interneurons reside (Fig. 2a, c).

Taken together, these in vivo results suggest that in utero electroporation could clearly label RMS at different developmental stages, and SVZa produces a unique source of cells destined to migrate through RMS into OB.

Morphology of SVZa Derived Cells in the OB

To observe the morphology of labeled cells, we used coronal and sagittal sections of OB. According to the layers distinguished by DAPI staining (Fig. 2b), EGFP-positive cells began to differentiate when they arrived their final position (Fig. 2b) and extended highly branched dendrites. As shown in Fig. 2a, 1', 2b, 2' (white arrow) the cell in the GCL had a characteristic morphology of granule cell: a small round soma and a long dendrite (with multiple branches at the tip) extending into the external plexiform layer. These cells distributed in different depths of GCL. Another typical morphology of neuron is periglomerular cell, as shown in Fig. 2a, 1', 2b, 2' (white arrowheads), which located at the border of the glomeruli, and had extensively branched dendrites within a single glomerulus.

Identity and Destiny of Labeled Cells In Vivo

To identify whether EGFP⁺ cells were RMS cells, immunostaining was performed. At P4, 9 days after electroporation of a GFP-expressing plasmid in E16 SVZa cells (E16-P4), the long longitudinal route from SVZa to SEZ in the OB was examined. As shown in Fig. 3a, b, e, most of these EGFP-positive cells were co-stained with Tuj-1, an immature neuronal marker, but not co-stained with GFAP, a marker of astrocytes. Most of EGFP-positive cells was also co-stained by anti-polysialylated neural cell adhesion molecule (PSA-NCAM) (Fig. 3a, c, e), which recognizes PSA portion of the high-molecular-weight neural cell adhesion molecule expressed in immature neurons (Oderfeld-Nowak

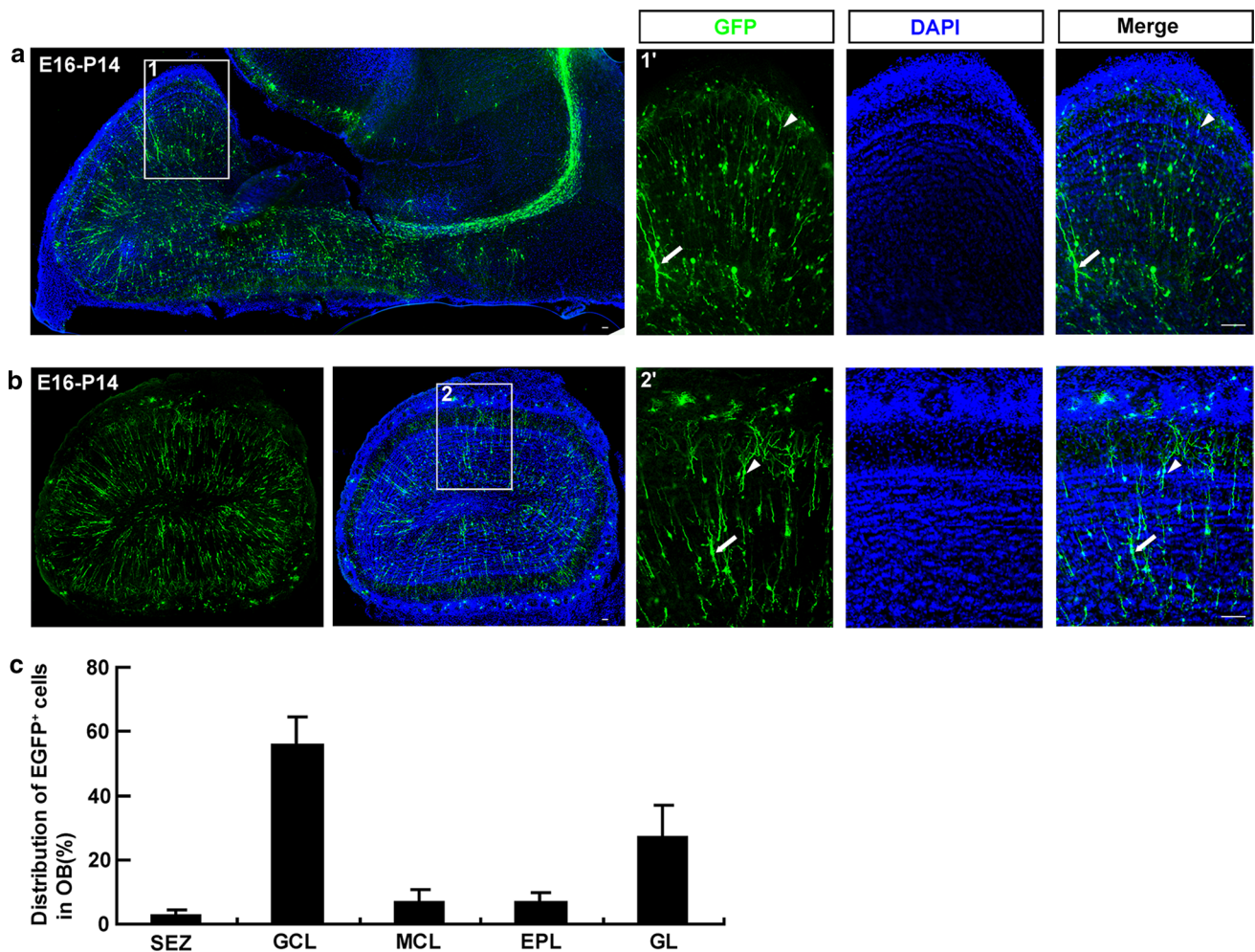


Fig. 2 Differentiation of SVZa derived cells in the OB. **a** Sagittal rat forebrain slice immunostained for GFP 19 days after electroporation of a GFP-expressing plasmid in E16 SVZa cells (E16-P14). **b** Horizontal rat OB slice immunostained for GFP 19 days after electroporation of a GFP-expressing plasmid in E16 SVZa cells (E16-P14). White arrow indicated the typical neurons in the GCL, and white

arrowheads indicated the typical neuron in periglomerular layer. **c** Quantification of GFP-positive cell distribution in OB as shown in **b** ($n = 10$). SEZ: subependymal zone; GCL: granule cell layer; EPL: external plexiform layer; GL: glomerular layer; OB: olfactory bulb; MCL: mitral cell layer. Scale bars, 100 μ m. Data were mean \pm sem

et al. 2009), partially with NG2 (Neuron/glia antigen 2) (Fig. 3a, c, e) and few with NeuN (mature neuronal marker) (Fig. 3a, c, e). In the GCL, EGFP-positive cells, expressed calbindin and GAD_{65/67} (Fig. 3d, e) suggest that these marked cells should be interneurons. These results suggest that labeled SVZa by in vivo electroporation could clearly trace RMS cells.

Progenitor Cells Generated at Postnatal Stages Migrate Faster than Embryonic Stages

Previous studies have shown that the major interneurons in the OB are derived from neuronal precursor cells from the lateral ganglionic eminences (LGE) in the embryonic stage (Wichterle et al. 2001) and continuously form the SVZa in

the postnatal stage (Luskin 1993; Lois et al. 1996). However, it is still unknown whether there are differences between at embryonic stages and postnatal stages in the motility of neuronal precursor cells. Here we used in utero electroporation to directly transfect EGFP plasmid into the anterior wall of the lateral ventricle at Embryonic 16 (E16) or P0. At P5, after 10 days injection at E16, most of the EGFP-positive cells migrated into the layers of OB (Fig. 4a, c). However, at P10, also after 10 days injection at P0, significantly higher percentage of EGFP-positive cells scattered into deeper layers of OB such as MCL, EPL, and GL; and significantly lower percentage distributed in the SVZ, RMS, and SEZ of OB (Fig. 4b, c, supplemental data Table 1). These indicated that the progenitor cell generated at postnatal stages might migrate faster than that generated at the embryonic stage.

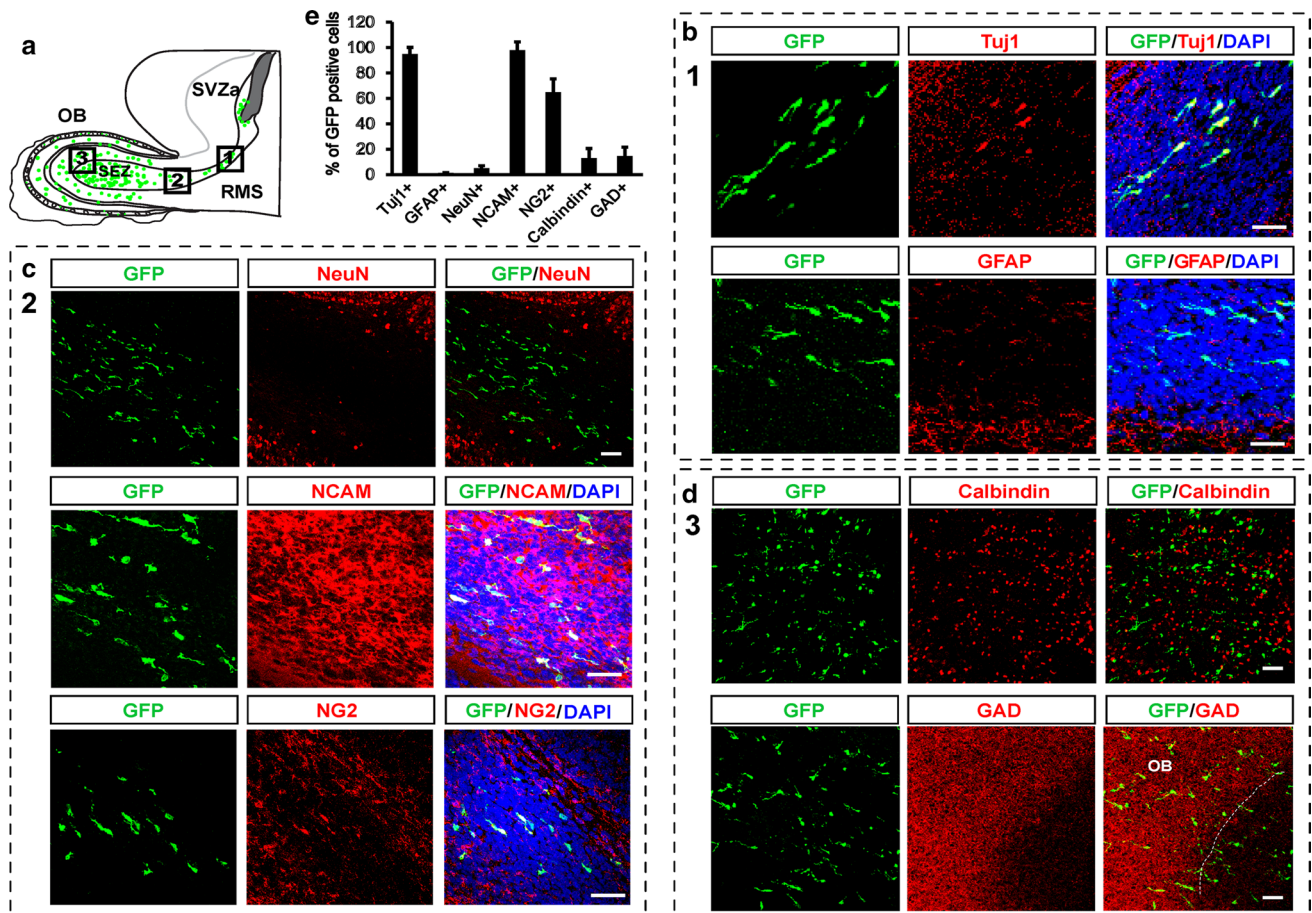


Fig. 3 Identity of labeled cells in vivo. **a** Illustration of selected fore-brain region for immunostaining at P4 rat, 9 days after electroporation of a GFP-expressing plasmid in E16 SVZa cells (E16-P4). **b** Double immunostaining of GFP (green) and Tuj1 (red) or GFP (green) and GFAP (red) in selected region 1 as shown in **a**. **c** Double immunostaining of GFP (green) and NeuN (red), or GFP (green) and

NCAM (red), or GFP (green) and NG2 (red) in selected region 2 as shown in **a**. **d** Double immunostaining of GFP (green) and Calbindin (red), or GFP (green) and GAD (red) in selected region 3 as shown in **a**. **e** Quantification of percentages of various markers and GFP-positive cells in total GFP-positive cells ($n = 10$ slides). Data were mean \pm sem. Scale bars, 50 μ m (Color figure online)

Migratory Properties of Neuroblasts in RMS

The tangential chain migration has been described as longitudinal clusters of neuroblasts that interact with each other. However, the exact migration rate and pattern were still unclear. To observe the migratory properties of neuroblasts in RMS, we performed time-lapse imaging experiments in slice cultures. Sagittal slices of P3 rat were used, after in vivo electroporation at P0. The injected pups were kept for 2 days to allow for EGFP expression. The EGFP signals were strong enough to visualize the long-distance translocating neurons from SVZ to the OB. Images were recorded in a time-lapse mode (3 h, 1 picture every 5 min).

Two migration modes were observed: one was the ‘branching cell movement’ (Fig. 5a, 1), where neuroblast exhibited typical migrating cell morphology with a small round cell body, one long leading process and a short trailing process at the onset. The cell first showed multipolar form

with branches, and branches were highly mobile looking for way. Then soma moved rapidly up to the branch point and retracted the processes. Another mode of migration was the ‘soma translocation’ migration (Fig. 5a, 2, 3 arrowhead), where neuroblasts had a straightly oriented leading process which was unbranched during the course of migration while maintaining a relatively constant length. Most of cells migrated forward from SVZ to OB; however, a few of cells migrated backward (Fig. 5a, 3 arrowhead). Analysis of their migration rate revealed that there was no significant difference between forward cells and backward cells (Fig. 5f).

The high motility in the formation and retraction of leading processes suggests that these migrating cells are actively exploring the environment for directional cues. And the transient stability of the leading process suggests that the direction of movement was predetermined temporarily. Although the migrating cells changed direction constantly or paused or even turned around, they strictly migrate forward in the

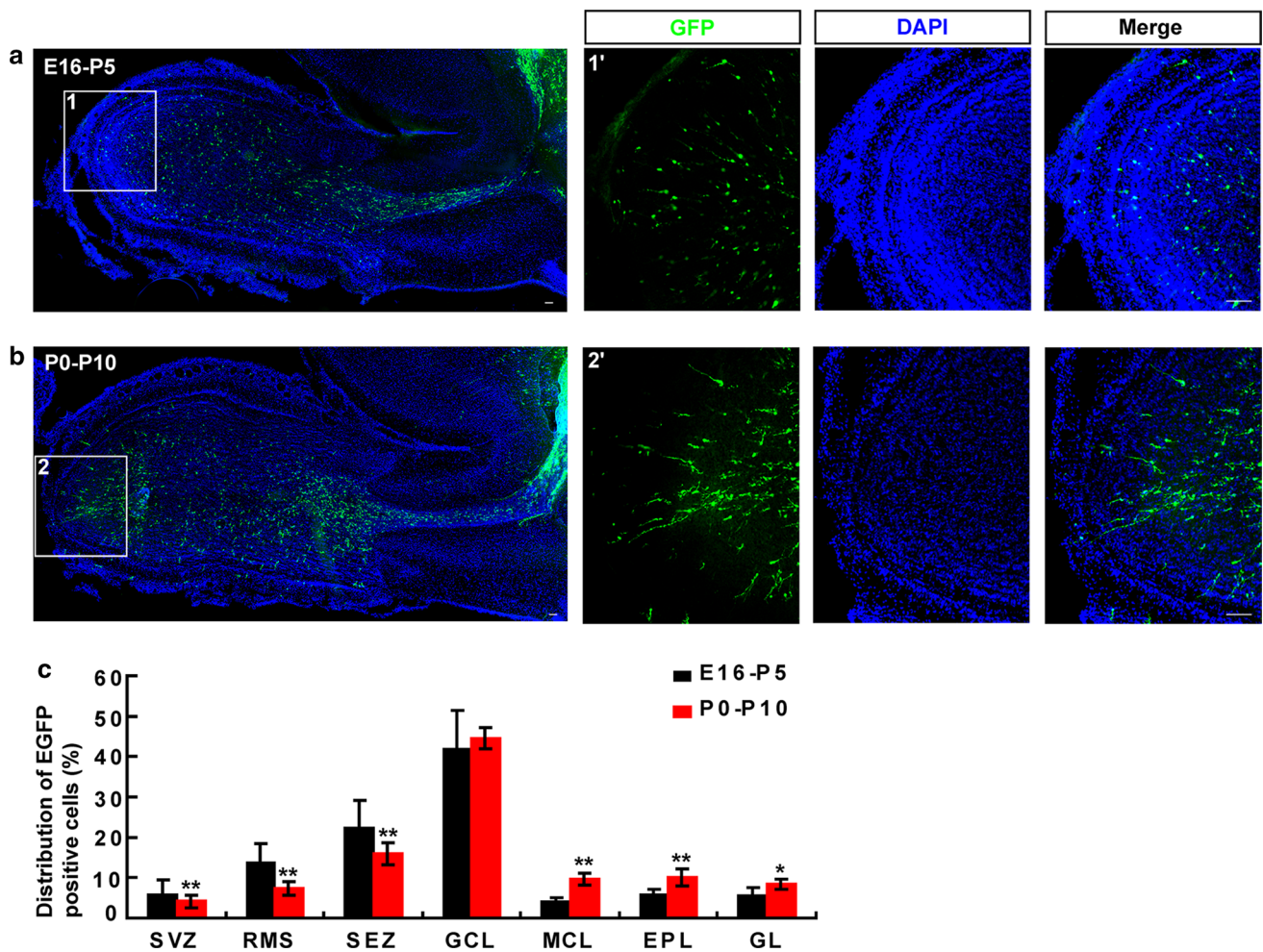


Fig. 4 Progenitor cells generated at postnatal ages migrated faster than those at embryonic ages. **a** Sagittal rat forebrain slice immunostained for GFP 10 days after electroporation of a GFP-expressing plasmid in E16 SVZa cells (E16-P5). **b** Sagittal rat forebrain slice immunostained for GFP 10 days after electroporation of a GFP-expressing plasmid in P0 SVZa cells (P0–P10). The selected regions (1, 2) were shown at higher magnification (1', 2'). **c** Quantification

of percentages of GFP-positive cells distribution in OB after electroporation of a GFP-expressing plasmid in E16 SVZa cells (E16-P5, $n = 14$) and in P0 SVZa cells (P0–P10, $n = 6$). Scale bars, 100 μm . Data were mean \pm SD. Statistical analysis was performed using Student's *t* test, ** $P < 0.01$, * $P < 0.05$, compared with each layer cells in OB after electroporation of a GFP-expressing plasmid in E16 SVZa cells (E16-P5), respectively

Table 1 Percentages of GFP-positive cells distribution in OB labeled at embryonic and postnatal ages

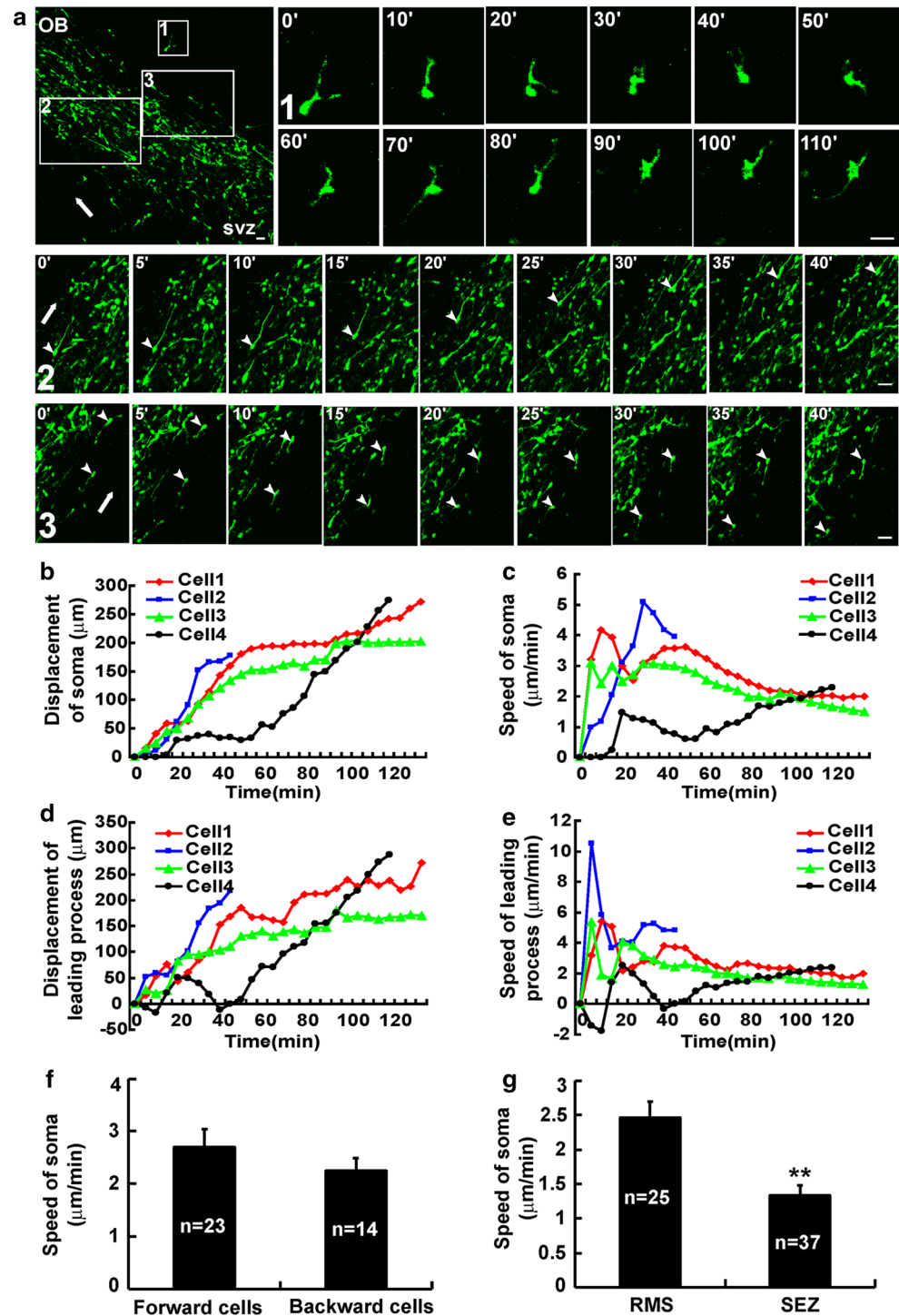
	SVZ (%)	RMS (%)	SEZ (%)	GCL (%)	MCL (%)	EPL (%)	GL (%)
E16-P5 ($n = 6$)	6.68 \pm 1.77	15.51 \pm 5.29	24.32 \pm 4.99	41.32 \pm 6.39	3.05 \pm 1.77	3.77 \pm 1.85	5.34 \pm 2.98
P0–P10 ($n = 14$)	4.12 \pm 1.55**	7.29 \pm 1.68**	15.91 \pm 2.66**	44.57 \pm 2.67	9.69 \pm 1.52**	10.07 \pm 2.08**	8.37 \pm 1.32*
<i>p</i>	0.0065	0.0017	0.0011	0.2500	2.630×10^{-7}	2.640×10^{-6}	0.0294

Data were mean \pm SD. Statistical analysis was performed using student's *t* test, ** $p < 0.01$, * $p < 0.05$, compared with each layer cells (SVZ, RMS, SEZ, GCL, MCL, EPL, and GL) in OB after electroporation of a GFP-expressing plasmid in E16 SVZa cells (E16-P5), respectively

RMS overall. Actually, these typical cells with higher motility in the RMS moved rapidly (soma, 2.145 $\mu\text{m}/\text{min}$; leading process, 2.671 $\mu\text{m}/\text{min}$, Fig. 5b–e). The velocity and direction of leading process changed a lot and always changed ahead of the soma movement (Fig. 5). Some cells such as

cell 4 migrated fast, and during observed time, this cell migrated out of the observed view, and then left a break line in graph (Fig. 5b–e). Analysis of their migration rate revealed that RMS cells migrated faster than SEZ cells (Fig. 5g). These results suggest that EGFP-labeled cells by

Fig. 5 Migratory properties of GFP-labeled cells in RMS pathways. **a** Time-lapse imaging of GFP-labeled cells in RMS pathways. After *in vivo* electroporation at P0, P3 sagittal rat forebrain slice was cultured. The selected regions (1, 2, and 3) were shown at higher magnification based on time-lapse imaging *in vivo*. White arrowheads indicated the direction of cell migration. **b–c** Quantitative analysis showed the migration distance **b** and speed **c** of soma of typical cells. **d–e** Quantitative analysis showed the migration distance **d** and speed **e** of leading process of typical cells ($n = 4$). White arrowheads indicated typical cells. **f–g** Quantitative analysis of average migration rate of cells as shown in **a**. Scale bars, 50 μm . Data were mean \pm sem. Statistical analysis was performed using Student's *t* test, $**p < 0.01$, compared with RMS cells



in vivo electroporation were suitable to time-lapse imaging study, and these cells displayed higher motility.

Migration of Neuronal Progenitor Cells From SVZa to OB was Affected by Extrinsic Environments

To examine whether migration of neuronal progenitor cells from SVZa to OB was affected by intrinsic or extrinsic

environments, tissue transplanted experiments were performed. EGFP-labeled SVZa tissues from P3 rat were transplanted into P0 OB brain slice, and 3 days after brain slice culture, these labeled cells could migrate diffusely into OB (Fig. 6a, b). Meanwhile, EGFP-labeled OB tissues from P3 mice were transplanted into P0 SVZa brain slice. Surprisingly, after 5 days brain slice culture, these labeled cells still could migrate into OB (Fig. 6a, c). These results suggest that

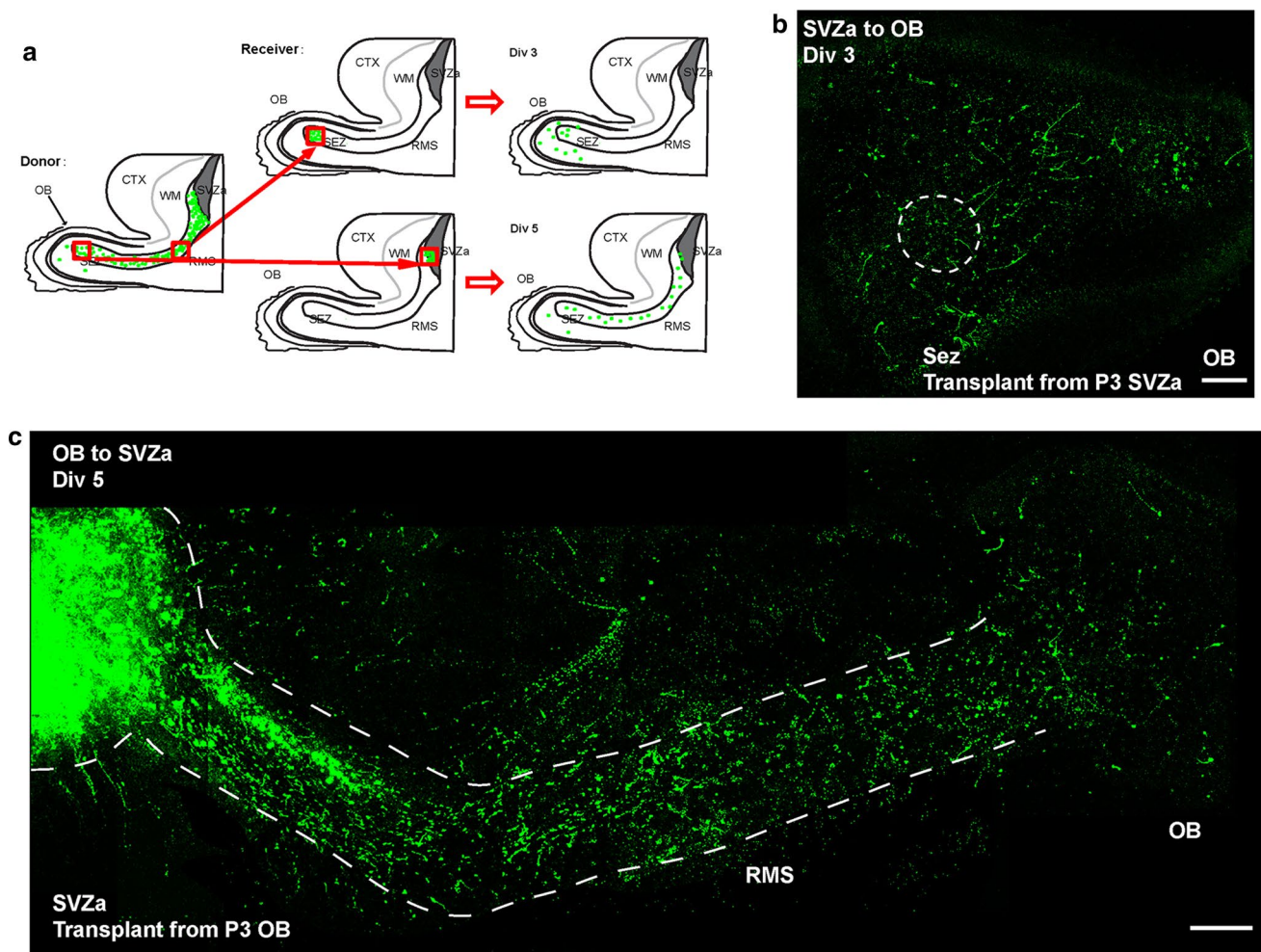


Fig. 6 Migration of neuronal progenitor cells from SVZa to OB was affected by extrinsic environments. **a** Illustration of transplantation experiments. GFP-labeled tissues were taken as hosts, and non-transfected tissues were taken as receivers. **b** Typical images showed

migration pattern of GFP-labeled SVZa tissues 3 days after transplanted into P0 OB. **c** Typical images showed migration pattern of GFP-labeled OB tissues 5 days after transplanted into P0 SVZa. Scale bars, 200 μ m

migration of neuronal progenitor cells from SVZa to OB was affected by extrinsic environments.

Discussion

The rostral migratory stream has been identified for decades; however, the detailed profile of this route and the molecular mechanisms remain unclear. In the present study, we developed *in vivo* electroporation to label the progenitor cells migrating through the RMS successfully, and pictured out the temporal-spatial migration and differentiation pattern of SVZa progenitor cells into the OB. In addition, with the transplant assay, we found migration in RMS was mainly affected by extrinsic environments.

The *in vivo* electroporation system was initially devised for use in chick embryos (Itasaki et al. 1999; Muramatsu

et al. 1997). Then many groups used developed *in utero* electroporation system, delivering plasmid into cortical neuron in developing embryos (Fukuchi-Shimogori and Grove 2001; Tabata and Nakajima 2001; Takahashi et al. 2002; Chen et al. 2008). Several previous studies have shown that *in vivo* electroporation also can label RMS of rodent olfactory system (Boutin et al. 2008; Chesler et al. 2008; Figueres-Onate and Lopez-Mascaraque 2016). Here we also developed this *in vivo* electroporation system which allows plasmid DNA to be introduced into neural progenitor cells at both the embryonic or postnatal stages, and studied the migratory properties of RMS of olfactory system based on this assay. Our studies showed that the strong EGFP fluorescence is sufficient to observe the morphology details of the labeled cells without immunohistochemistry, and enables the entire processes and route of the migration to be visualized in real time. This assay is efficient for the gain or loss of

function of gene manipulations on the mammals, compared to BrdU administration and dye injection experiments. The role of any gene involved in these processes can be easily evaluated by overexpression of these proteins or their mutants, or knock-down of their genes by RNA interference (Belvindrah et al. 2011; Sonogo et al. 2015; 2013a). In addition, it is capable of regulate gene expression in the certain cell population which could not only avoid early embryonic lethality by conventional transgenic techniques, and also the cross influence by other cells such as glia cells. Thus, based on time-lapse imaging and brain slice culture system, this assay may be applied in future in the following fields as a powerful tool to study the migratory properties and molecular mechanisms of neuroblasts of RMS: 1) analyze the migratory properties of embryonically labeled precursor cells in comparison with postnatally labeled ones in more detail; 2) explore the potential functions of interest genes in neuroblast migration based on electroporation of shRNA or over-expressing plasmids or Cre recombinase-expressing plasmids in conditional knockout mice employing LoxP system; and 3) investigate the detail roles of different signaling molecules in neuroblast migration by pharmacological manipulation of acute brain slice cultures.

It was assumed that the adult SVZ is derived from the lateral ganglionic eminence (LGE) of the embryonic telencephalon. The LGE progenitors grafted into the LGE or adult SVZ produce neuroblasts that migrate to the OB (Wichterle et al. 2001). Here our studies showed that plasmid injected into the anterior part of lateral ventricle which is just above the vertical limb of the RMS, and received a voltage pulse anterior-posteriorly, could effectively be introduced into the progenitors that migrate into the RMS. If the plasmid was introduced into the later ventricle at E16 but received a voltage pulse ventral-dorsally, the labeled cells would migrate into cortical cortex (Borrell et al. 2005; LoTurco et al. 2009). That means the origin of the embryonic OB neurons is specifically localized and could be traced.

Previous studies have showed that the peak of OB interneuron production occurs in the first postnatal week in mice (Alvarez-Buylla and Lim 2004). Interneurons born during the early period appear more likely to differentiate and survive long term in the OB than interneurons generated later (Lemasson et al. 2005; Magavi et al. 2005; Plachez and Puche 2012; Parrish-Aungst et al. 2007). However, the existing results are restricted at early neonatal stages like P3 to P7, but our studies traced the development of interneurons generated as early as E16, using the in utero electroporation technique. These labeled neurons could be traced for long time (more than 3 weeks), and reached into different layers of OB. Consistent with previous studies (Boutin et al. 2008; Sonogo et al. 2015; 2013b), these neurons could finally become into mature neurons such as granule neurons and periglomerular neurons (Fig. 2). These results suggest that

this assay can successfully trace neurons of RMS. Additionally, the progenitor cells generated at postnatal stage (P0) migrate into more exterior layers in the OB than those generated at the embryonic stage (E16). Our data showed that the cells generated at P0 migrate faster than the cells generated at E16, according to the percentage of cells in the different layers of OB (including SEZ, GCL, MCL, EPL, and GL); even the migration routes from SVZ to OB is shorter at the embryonic stages than the postnatal stages. In addition, the P0 generated cells penetrated into the outer layers of the OB such as MCL, EPL, and GL, but not SEZ. It is possible that once the cell changed into radial migration mode after enter the OB, the later generated cells tended to penetrated into the upper layers, just like the inside-out pattern in radial migration of cortical neurons (Hatanaka et al. 2004). This suggests that interneurons generated at different development stages might be involved into different OB circuits, and this is important for odor discrimination. The interneuron migration and lamination into OB is not strictly age-dependent as cortical neuron in the cortical cortex, since the E16-derived cells also could penetrate into the GL layer, but with a smaller proportion. The robust migration of neural progenitors in the embryonic and early postnatal stages suggests the importance of maintain a high level of functional synaptic plasticity at this crucial stage of neural development.

It has been observed in vitro that the RMS cells migrate on the surface of the adjacent RMS cells, which serve as a migratory scaffolding (Lois et al. 1996; Rousselot et al. 1995). However, we also observed the chain formation in our in vivo system. The migrating cells are the interconnected with each other, but not rely on other cell types. The migrating cell has a long leading process, with a large growth cone. We also found that the neuroblasts in RMS migrate very rapidly along one another at the rate of 2.145 $\mu\text{m}/\text{min}$ and the leading processes move even faster at the rate of 2.671 $\mu\text{m}/\text{min}$, which is consistent with the velocity found in the culture systems, which is 2.033 $\mu\text{m}/\text{min}$ (Wichterle et al. 1997), and significantly faster than at the rate of 0.33–0.5 $\mu\text{m}/\text{min}$ in vivo studies by X-Gal staining (Luskin and Boone 1994) or dye tracing (Lois and Alvarez-Buylla 1994), or slice cultures by dye tracing (Bovetti et al. 2007). These rates are dramatically faster (2–8 times) than those reported of other tangential migrations, e.g., precursors of cortical interneurons derived from medial ganglionic eminence (0.967 $\mu\text{m}/\text{min}$) (Polleux et al. 2002) or granule cell precursors in the cerebellum (0.25 $\mu\text{m}/\text{min}$) (Komuro et al. 2001). These different results may be due to different study systems (such as time-lapse imaging based on slice culture VS in vivo tracing).

Some migrating neural cells migrate as ‘soma translocation’ mode, which is a characteristic biphasic pattern of movement. This soma translocation contains typical nucleokinesis, where the leading process elongate towards and

then followed by nuclear translocation. Nucleokinesis is frequently preceded by transient thickening of the proximal leading processes (Schaar and McConnell 2005), and this was clearly observed in our time-lapse studies (Fig. 5). Another interesting migration type is the ‘branching cell movement’ mode. The cells could change from bipolar into multipolar freely and the leading process could branch and turn in a high dynamic. This mode is important since the migrating neurons are influenced by the microenvironment in which they reside or have migrated through. However, we never observed cells spontaneously turned 90° to emigrate radially from the SVZ. This indicates that some structural and/or chemical boundary between the SVZ and adjacent structures could restrict neuronal progenitor migration; maybe it was the contribution of astrocyte ‘tunnel’ array around the certain route with a strong GFAP-positive signal (Fig. 3).

It was assumed that neuroblasts have an intrinsic capacity to migrate (Lledo et al. 2008) even when they are isolated from their native environment, since the chain migration can be recapitulated *in vitro* by embedding RMS explants in a three-dimensional Matrigel matrix (Lindberg et al. 2012). Moreover, previous study has shown that progenitor cells isolated from the LGE or SVZ at different stages (embryonic day 15 and postnatal days 2 and 30) engraft into the SVZ of neonatal or adult mice, migrate to the OB, and differentiate into local interneurons, including granule and periglomerular cells as well as other types of interneurons (De Marchis et al. 2007). Similarly, we transplanted the cells migrating in the RMS limb forward into SEZ; the cells could migrate radially into different layers of the OB, but not migrate tangentially like the cells in the RMS (Fig. 6). Interestingly, the cells (that already migrated in SEZ of OB) were transplanted back into RMS, the cells could still migrate out tangentially along the RMS to OB as the cells generated from SVZa (Fig. 6). These results suggest that migration of neuronal progenitor cells from SVZa to OB was also affected by extrinsic environments. Further studies will be carried out to confirm this phenotype and examine related molecular mechanisms in future.

In conclusion, with the appropriate injection site and direction of electric pulse, we developed an *in vivo* electroporation technic, which could label a certain type of neuroblasts in SVZa efficiently at both embryonic and neonatal stages. These labeled SVZa progenitors migrated into the OB through rostral migratory stream including tangential and radial migration. Additionally, the migration route and mode of RMS was mainly regulated also by extrinsic environments. Interestingly, the postnatal generated cells migrate faster than the embryonic ones. Our studies will provide a powerful tool and some insights to understand the migratory properties and molecular mechanisms of neuroblasts in RMS at embryonic and postnatal ages.

Acknowledgements We acknowledge that this study was funded by the several grants as follows: Zhejiang Provincial Natural Science Foundation of China under Grant (LY15C090006, Q17H090034, R18C090008), Science and Technology Planning Project of Zhejiang Province (2017C33197), National Natural Science Foundation (3167107, 181371350), and the Outstanding Leaders Training Program of Pudong Health Bureau of Shanghai (NO. PWR12015-06).

Author Contributions ZHH and YW planned the study, wrote the main manuscript, and performed the main experiments. YWX, ZYL, JD, and TTW performed staining experiments. SXH, YC, and BYC were responsible for the cultivation of experiments, providing general coordination of the study, and revised the manuscript. All authors have read and approved the final manuscript.

Compliance with Ethical Standards

Conflict of interest The authors declare that there is no conflict of interest.

Ethical Approval All applicable international, national, and institutional guidelines for the care and use of animals were followed.

References

- Alvarez-Buylla A, Lim DA (2004) For the long run: maintaining germinal niches in the adult brain. *Neuron* 41(5):683–686
- Ayala R, Shu T, Tsai LH (2007) Trekking across the brain: the journey of neuronal migration. *Cell* 128(1):29–43
- Bakhshetyan K, Saghatelian A (2015) Tracking neuronal migration in adult brain slices. *Current Protoc Neurosci*. <https://doi.org/10.1002/0471142301.ns0328s71>
- Belvindrah R, Nissant A, Lledo PM (2011) Abnormal neuronal migration changes the fate of developing neurons in the postnatal olfactory bulb. *J Neurosci* 31(20):7551–7562. <https://doi.org/10.1523/JNEUROSCI.6716-10.2011>
- Borrell V, Yoshimura Y, Callaway EM (2005) Targeted gene delivery to telencephalic inhibitory neurons by directional *in utero* electroporation. *J Neurosci Methods* 143(2):151–158. <https://doi.org/10.1016/j.jneumeth.2004.09.027>
- Boutin C, Diestel S, Desoeuvre A, Tiveron MC, Cremer H (2008) Efficient *in vivo* electroporation of the postnatal rodent forebrain. *PLoS ONE* 3(4):e1883. <https://doi.org/10.1371/journal.pone.0001883>
- Bovetti S, Bovolin P, Perroteau I, Puche AC (2007) Subventricular zone-derived neuroblast migration to the olfactory bulb is modulated by matrix remodelling. *The Eur j neurosci* 25(7):2021–2033. <https://doi.org/10.1111/j.1460-9568.2007.05441.x>
- Chen G, Sima J, Jin M, Wang KY, Xue XJ, Zheng W, Ding YQ, Yuan XB (2008) Semaphorin-3A guides radial migration of cortical neurons during development. *Nat Neurosci* 11(1):36–44. <https://doi.org/10.1038/nn2018>
- Chesler AT, Le Pichon CE, Brann JH, Araneda RC, Zou DJ, Firestein S (2008) Selective gene expression by postnatal electroporation during olfactory interneuron neurogenesis. *PLoS ONE* 3(1):e1517. <https://doi.org/10.1371/journal.pone.0001517>
- Coskun V, Luskin MB (2002) Intrinsic and extrinsic regulation of the proliferation and differentiation of cells in the rodent rostral migratory stream. *J Neurosci Res* 69(6):795–802. <https://doi.org/10.1002/jnr.10336>
- De Marchis S, Bovetti S, Carletti B, Hsieh YC, Garzotto D, Peretto P, Fasolo A, Puche AC, Rossi F (2007) Generation of

- distinct types of periglomerular olfactory bulb interneurons during development and in adult mice: implication for intrinsic properties of the subventricular zone progenitor population. *J Neurosci* 27(3):657–664. <https://doi.org/10.1523/JNEUROSCI.2870-06.2007>
- Dixon KJ, Turbic A, Turnley AM, Liebl DJ (2017) Explant methodology for analyzing neuroblast migration. *Bio-protocol*. <https://doi.org/10.21769/BioProtoc.2249>
- Ernst A, Alkass K, Bernard S, Salehpour M, Perl S, Tisdale J, Posner G, Druid H, Frisen J (2014) Neurogenesis in the striatum of the adult human brain. *Cell* 156(5):1072–1083. <https://doi.org/10.1016/j.cell.2014.01.044>
- Fasolo A, Peretto P, Bonfanti L (2002) Cell migration in the rostral migratory stream. *Chem Senses* 27(6):581–582
- Figueres-Onate M, Lopez-Masaraque L (2016) Adult olfactory bulb interneuron phenotypes identified by targeting embryonic and postnatal neural progenitors. *Front Neurosci* 10:194. <https://doi.org/10.3389/fnins.2016.00194>
- Fukuchi-Shimogori T, Grove EA (2001) Neocortex patterning by the secreted signaling molecule FGF8. *Science* 294(5544):1071–1074. <https://doi.org/10.1126/science.1064252>
- Hatanaka Y, Hisanaga S, Heizmann CW, Murakami F (2004) Distinct migratory behavior of early- and late-born neurons derived from the cortical ventricular zone. *J Comp Neurol* 479(1):1–14. <https://doi.org/10.1002/cne.20256>
- Itasaki N, Bel-Vialar S, Krumlauf R (1999) ‘Shocking’ developments in chick embryology: electroporation and in ovo gene expression. *Nat Cell Biol* 1(8):E203–207. <https://doi.org/10.1038/70231>
- Kaneko N, Sawada M, Sawamoto K (2017) Mechanisms of neuronal migration in the adult brain. *J Neurochem* 141(6):835–847. <https://doi.org/10.1111/jnc.14002>
- Komuro H, Yacubova E, Rakic P (2001) Mode and tempo of tangential cell migration in the cerebellar external granular layer. *J Neurosci* 21(2):527–540
- Kulesa PM, Fraser SE (2000) In ovo time-lapse analysis of chick hind-brain neural crest cell migration shows cell interactions during migration to the branchial arches. *Development* 127(6):1161–1172
- Lalli G (2014) Extracellular signals controlling neuroblast migration in the postnatal brain. *Adv Exp Med Biol* 800:149–180. https://doi.org/10.1007/978-94-007-7687-6_9
- Lemasson M, Saghatelian A, Olivo-Marin JC, Lledo PM (2005) Neonatal and adult neurogenesis provide two distinct populations of newborn neurons to the mouse olfactory bulb. *J Neurosci* 25(29):6816–6825. <https://doi.org/10.1523/JNEUROSCI.1114-05.2005>
- Lindberg OR, Persson A, Brederlau A, Shabro A, Kuhn HG (2012) EGF-induced expansion of migratory cells in the rostral migratory stream. *PLoS ONE* 7(9):e46380. <https://doi.org/10.1371/journal.pone.0046380>
- Lledo PM, Merkle FT, Alvarez-Buylla A (2008) Origin and function of olfactory bulb interneuron diversity. *Trends Neurosci* 31(8):392–400. <https://doi.org/10.1016/j.tins.2008.05.006>
- Lois C, Alvarez-Buylla A (1994) Long-distance neuronal migration in the adult mammalian brain. *Science* 264(5162):1145–1148
- Lois C, Garcia-Verdugo JM, Alvarez-Buylla A (1996) Chain migration of neuronal precursors. *Science* 271(5251):978–981
- LoTurco J, Manent JB, Sidiqi F (2009) New and improved tools for in utero electroporation studies of developing cerebral cortex. *Cereb Cortex* 19(Suppl 1):i120–125. <https://doi.org/10.1093/cercor/bhp033>
- Luskin MB (1993) Restricted proliferation and migration of postnatally generated neurons derived from the forebrain subventricular zone. *Neuron* 11(1):173–189
- Luskin MB, Boone MS (1994) Rate and pattern of migration of lineally-related olfactory bulb interneurons generated postnatally in the subventricular zone of the rat. *Chem Senses* 19(6):695–714
- Luskin MB, Zigova T, Soteres BJ, Stewart RR (1997) Neuronal progenitor cells derived from the anterior subventricular zone of the neonatal rat forebrain continue to proliferate in vitro and express a neuronal phenotype. *Mol Cell Neurosci* 8(5):351–366. <https://doi.org/10.1006/mcne.1996.0592>
- Magavi SS, Mitchell BD, Szentirmai O, Carter BS, Macklis JD (2005) Adult-born and preexisting olfactory granule neurons undergo distinct experience-dependent modifications of their olfactory responses in vivo. *J Neurosci* 25(46):10729–10739. <https://doi.org/10.1523/JNEUROSCI.2250-05.2005>
- Martinez-Molina N, Kim Y, Hockberger P, Szele FG (2011) Rostral migratory stream neuroblasts turn and change directions in stereotypic patterns. *Cell Adh Migr* 5(1):83–95
- Muramatsu T, Mizutani Y, Ohmori Y, Okumura J (1997) Comparison of three nonviral transfection methods for foreign gene expression in early chicken embryos in ovo. *Biochem Biophys Res Commun* 230(2):376–380
- Oderfeld-Nowak B, Zaremba M, Kwiatkowska-Patzer B, Lipkowski AW, Kurkowska-Jastrzebska I, Triaca V, Aloe L (2009) NG2 positive cells of rat spinal cord activated during experimental autoimmune encephalomyelitis are spatially associated with radially oriented astroglia and express p75 receptor: a role for nerve growth factor in oligodendrocyte progenitor migration? *Arch Ital Biol* 147(4):105–115
- Omori K, Asai M, Kuga D, Ushida K, Izuchi T, Mii S, Enomoto A, Asai N, Nagino M, Takahashi M (2015) Girdin is phosphorylated on tyrosine 1798 when associated with structures required for migration. *Biochem Biophys Res Commun* 458(4):934–940. <https://doi.org/10.1016/j.bbrc.2015.02.065>
- Parrish-Aungst S, Shipley MT, Erdelyi F, Szabo G, Puche AC (2007) Quantitative analysis of neuronal diversity in the mouse olfactory bulb. *J Comp Neurol* 501(6):825–836. <https://doi.org/10.1002/cne.21205>
- Pencea V, Bingaman KD, Freedman LJ, Luskin MB (2001) Neurogenesis in the subventricular zone and rostral migratory stream of the neonatal and adult primate forebrain. *Exp Neurol* 172(1):1–16. <https://doi.org/10.1006/exnr.2001.7768>
- Persson A, Lindberg OR, Kuhn HG (2013) Radixin inhibition decreases adult neural progenitor cell migration and proliferation in vitro and in vivo. *Frontiers Cell Neurosci* 7:161. <https://doi.org/10.3389/fncel.2013.00161>
- Plachez C, Puche AC (2012) Early specification of GAD67 subventricular derived olfactory interneurons. *J Mol Histol* 43(2):215–221. <https://doi.org/10.1007/s10735-012-9394-2>
- Polleux F, Whitford KL, Dijkhuizen PA, Vitalis T, Ghosh A (2002) Control of cortical interneuron migration by neurotrophins and PI3-kinase signaling. *Development* 129(13):3147–3160
- Rousselot P, Lois C, Alvarez-Buylla A (1995) Embryonic (PSA) N-CAM reveals chains of migrating neuroblasts between the lateral ventricle and the olfactory bulb of adult mice. *J Comp Neurol* 351(1):51–61. <https://doi.org/10.1002/cne.903510106>
- Sakamoto M, Kageyama R, Imayoshi I (2014) The functional significance of newly born neurons integrated into olfactory bulb circuits. *Front Neurosci* 8:121. <https://doi.org/10.3389/fnins.2014.00121>
- Sanai N, Nguyen T, Ihrig RA, Mirzadeh Z, Tsai HH, Wong M, Gupta N, Berger MS, Huang E, Garcia-Verdugo JM, Rowitch DH, Alvarez-Buylla A (2011) Corridors of migrating neurons in the human brain and their decline during infancy. *Nature* 478(7369):382–386. <https://doi.org/10.1038/nature10487>
- Schaar BT, McConnell SK (2005) Cytoskeletal coordination during neuronal migration. *Proc Natl Acad Sci USA* 102(38):13652–13657. <https://doi.org/10.1073/pnas.0506008102>
- Sonego M, Gajendra S, Parsons M, Ma Y, Hobbs C, Zentar MP, Williams G, Machesky LM, Doherty P, Lalli G (2013a) Fascin regulates the migration of subventricular zone-derived neuroblasts in

- the postnatal brain. *J Neurosci* 33(30):12171–12185. <https://doi.org/10.1523/JNEUROSCI.0653-13.2013>
- Sonego M, Zhou Y, Oudin MJ, Doherty P, Lalli G (2013b) In vivo postnatal electroporation and time-lapse imaging of neuroblast migration in mouse acute brain slices. *J Vis Exp*. <https://doi.org/10.3791/50905>
- Sonego M, Oberoi M, Stoddart J, Gajendra S, Hendricusdottir R, Oozeer F, Worth DC, Hobbs C, Eickholt BJ, Gordon-Weeks PR, Doherty P, Lalli G (2015) Drebrin regulates neuroblast migration in the postnatal mammalian brain. *PLoS ONE* 10(5):e0126478. <https://doi.org/10.1371/journal.pone.0126478>
- Tabata H, Nakajima K (2001) Efficient in utero gene transfer system to the developing mouse brain using electroporation: visualization of neuronal migration in the developing cortex. *Neuroscience* 103(4):865–872
- Takahashi M, Sato K, Nomura T, Osumi N (2002) Manipulating gene expressions by electroporation in the developing brain of mammalian embryos. *Differentiation* 70(4–5):155–162. <https://doi.org/10.1046/j.1432-0436.2002.700405.x>
- Wichterle H, Garcia-Verdugo JM, Alvarez-Buylla A (1997) Direct evidence for homotypic, glia-independent neuronal migration. *Neuron* 18(5):779–791
- Wichterle H, Turnbull DH, Nery S, Fishell G, Alvarez-Buylla A (2001) In utero fate mapping reveals distinct migratory pathways and fates of neurons born in the mammalian basal forebrain. *Development* 128(19):3759–3771